A Multimode/Multiband Envelope Tracking Transmitter with Broadband Saturated Power Amplifier

Junghwan Moon, Junghwan Son, Juyeon Lee, Jungjoon Kim,
Seunghoon Jee, Seungchan Kim, and Bumman Kim

Department of Electrical Engineering and Division of Information Technology Convergence Engineering,
Pohang University of Science and Technology (POSTECH),
Gyeongbuk, 790-784, Republic of Korea, Tel: +82-54-279-5584, Fax: +82-54-279-8115
E-mail: {jhmoon, bmkim}@postech.edu

***Abstract*— A multimode/multiband envelope tracking (ET) transmitter consisting of a hybrid switching amplifier (HSA) and a broadband saturated power amplifier (PA) is developed across 1.3 to 2.7 GHz. For the various standard signals with different bandwidth and peak-to-average power ratio, the HSA efficiently provides a supply signal to the PA by changing the reference value of the hysteresis comparator. The broadband saturated PA, taking advantage of a nonlinear output capacitor to shape the voltage waveform, is implemented based on load/source-pull methodology. Broadband matching networks for the high efficiency are synthesized by simplified real frequency technique. For the bandwidth from 1.3 to 2.7 GHz (70% fractional bandwidth), the measured output power, drain efficiency, and power-added efficiency (PAE) performances are between 39.8–42.0 dBm, 55.8–69.7%, and 51.2–65.3%, respectively. The ET transmitter is demonstrated at 1.8425-GHz long-term evolution (LTE), 2.14-GHz wideband code division multiple access (WCDMA), and 2.6-GHz mobile world wide interoperability for microwave access (m-WiMAX) applications. It delivers the PAE of 32.16, 37.24, and 28.75% for LTE, WCDMA, and m-WiMAX applications, which are improved by 3.1, 4.2, and 1.7%, respectively.**

***Index Terms*— Broadband power amplifier (PA), envelope tracking, multiband, multimode.**

I. Introduction

As wireless communication systems evolve, signals of the systems such as long-term evolution (LTE), mobile world wide interoperability for microwave access (m-WiMAX), and wideband code division multiple access (WCDMA) have wideband characteristic and high peak-to-average power ratio (PAPR). From the transmitter point of view, power amplifiers (PAs) of the systems should linearly amplify the signals, leading to operation in back-off region and low amplification efficiency. Moreover, increasing number of frequency bands and spectrum fragmentation require development of circuits and subsystems having broadband capabilities [1]–[10].

To efficiently amplify the signals, the Doherty and envelope tracking (ET) PAs have been extensively investigated. The Doherty PA modulates the load according to the power level using a quarter-wavelength transformer. However, this transformer is sensitive to the frequency, thus preventing broadband operation. On the other hand, ET technique with a broadband PA enables the multiband operation because the supply modulator such as a hybrid switching amplifier (HSA) is independent on the operating frequency [1]–[4].

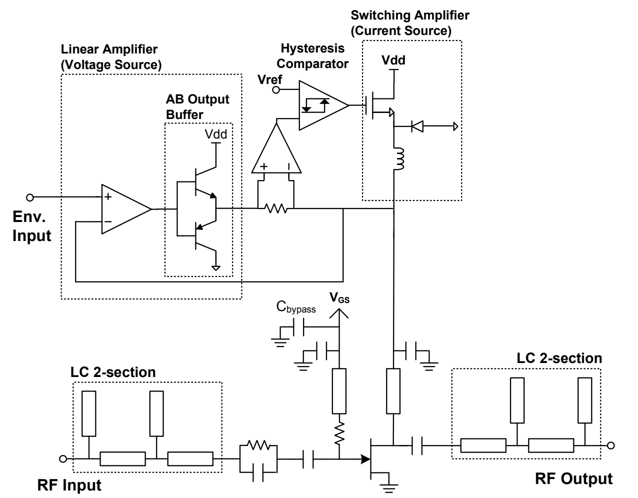

Fig. 1. Multimode/multiband ET transmitter with a broadband saturated amplifier.

In this paper, a high efficiency multimode/multiband ET PA is developed using a HSA and a broadband saturated PA. For the various standards with different signal bandwidths and PAPRs, the HSA provide a supply voltage with high efficiency by adopting the proper reference value of the hysteresis comparator [3]. The saturated PA can deliver high efficiency due to the nonlinear output capacitor [5]. This capacitor enables highly efficient operation across the broadband without any special harmonic control circuitry. Broadband source and load impedances are found by load/source-pull methodology, then synthesized using simplified real frequency technique (SRFT) across 1.3 to 2.7 GHz [6]. The multimode/multiband ET PA is demonstrated at 1.8425-GHz LTE, 2.14-GHz WCDMA, and 2.6-GHz m-WiMAX applications.

II. Design of Multimode/Multiband Envelope Tracking Transmitter

Fig. 1 shows the architecture of the multimode/multiband ET transmitter consisting of a HSA and a broadband saturated amplifier. The highly efficient HSA includes a linear stage and

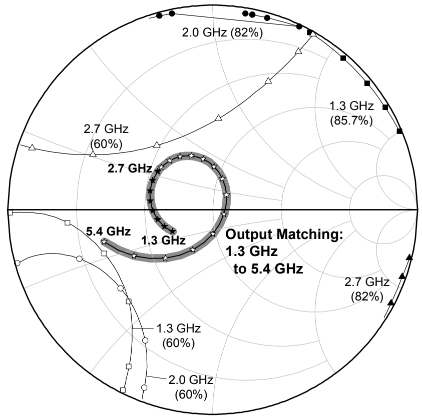

(a)

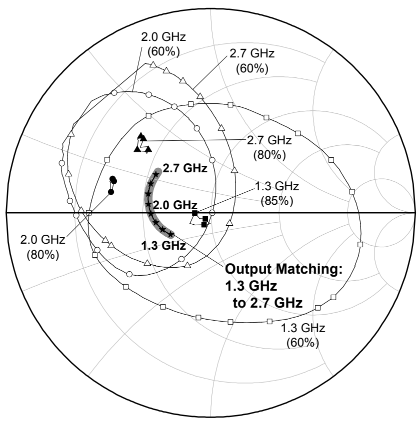

(b)

Fig. 2. Simulated (a) second harmonic and (b) fundamental load-pull contours for the achievable efficiencies of 60% at 1.3, 2.0, and 2.7 GHz.

an efficient switcher stage to efficiently and linearly provide the supply voltage to the power amplifier. A buck converter is used as the switch, efficiently providing most of the current required for the amplifier. In the linear stage, an OP amplifier and class-AB output buffer linearly amplify the envelope voltage applied to the PA.

In this architecture, the saturated amplifier is employed, its voltage shaping is carried out by the nonlinear output capacitor of the power transistor, thus improving the efficiency [5]. In general, the nonlinear output capacitance, consisting of drain-source and gate-drain capacitors, changes according to the drain-source voltage. As the drain-source voltage decreases, the capacitance increases rapidly. Thus, the voltage across the capacitor has the half-sinusoidal waveform except when the second harmonic impedance is near short-circuit region or conjugate level of the reactance of the output capacitor. The behavior of the output capacitor enables the broadband operation with high efficiency because it is not required to make an effort to carefully manipulate the harmonic load impedance. In this work, the broadband amplifier is designed using CREE GaN HEMT CGH40010 device and with a goal of above 60% efficiency over the 70% bandwidth from 1.3

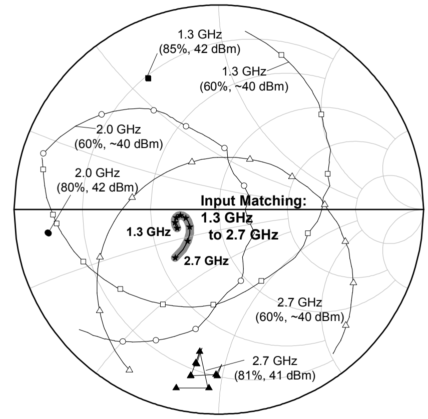

Fig. 3. Simulated fundamental source-pull contours for the achievable efficiencies of 60% at 1.3, 2.0, and 2.7 GHz.

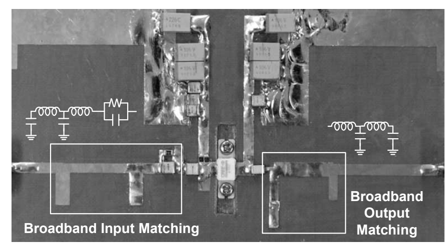

Fig. 4. Photo of the designed broadband saturated amplifier.

to 2.7 GHz. Fig. 2(a) shows the simulated second harmonic load-pull contours for the achievable efficiencies of 60% at 1.3, 2.0, and 2.7 GHz. As shown, the high efficiency can be obtained for the broad region of the second harmonic load and the careful matching for the fundamental load is the most important procedure. Fig. 2(b) shows the simulated fundamental load-pull contours for the achievable efficiencies. During the simulation, the second harmonic loads are set to 1000 Ω. With the targeted fundamental load impedances across the bandwidth, the output matching network is designed using SRFT [6]. During the synthesis, 2-section low-pass LC network is employed for the matching network. The resulting LC elements from the SRFT is then converted to the distributed network. The matching impedance generated by the SRFT is overlaid with the load-pull contours in Fig. 2. The resulting load impedances across the frequency band from 1.3 to 5.4 GHz are within the high efficiency region. An analogous procedure has been used for the input matching network, and this is described in Fig. 3. During the source-pull simulation, the parallel RC network is attached at the transistor's gate-terminal, as shown in Fig. 1, to provide the flat gain response and stable operation across the targeted bandwidth. The resulting source impedances synthesized by the SRFT are also overlaid with the source-pull contours as shown in Fig. 3.

III. Implementation and Experimental Results

The broadband saturated amplifier is fabricated as shown in Fig. 4. This amplifier is implemented on a Taconic TLY-

978-1-61284-757-3/11/$26.00 C2011 IEEE

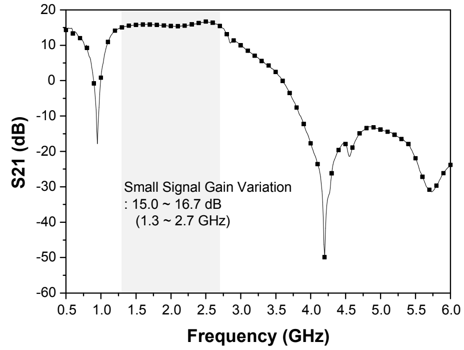

Fig. 5. Measured small-signal gain of the designed amplifier.

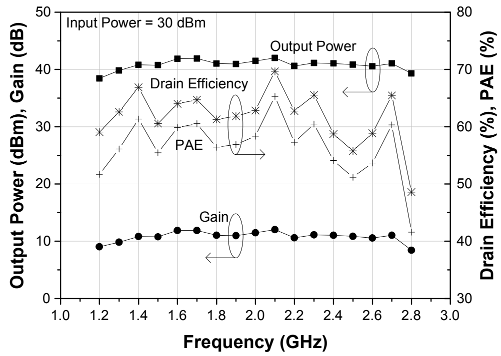

Fig. 6. Measured output power, gain, efficiency, and PAE of the implemented amplifier across the bandwidth from 1.2 to 2.8 GHz.

5 substrate with $\varepsilon_r = 2.2$ and thickness of 31 mil. In the experiment, the drain bias and the idle current are set to $V_{DS} = 30$ V and $I_{DSQ} = 200$ mA, respectively. Fig. 5 shows the measured small-signal gain characteristic of the implemented amplifier. For the targeted bandwidth from 1.3 to 2.7 GHz, the gain is between 15.0–16.7 dB. The broadband amplifier is characterized using a constant input power of 30 dBm, as shown in Fig. 6. The measured output power, drain efficiency (DE), and PAE performances are between 39.8–42.0 dBm, 55.8–69.7%, and 51.2–65.3%, respectively, in the frequency range of 1.3 to 2.7 GHz. The performances are summarized in Table I together with state-of-the-art broadband PAs.

The multimode/multiband ET operations are demonstrated

TABLE I
STATE-OF-THE-ART BROADBAND PAS

Ref.	BW (GHz / %)	P_{out} (dBm)	Gain (dB)	DE (%)
[6]	1.90−2.90 / 42	45.0−47.0	10−12	60.0−65.0
[7]	1.90−4.30 / 78	40.0−42.0	9−11	57.0−72.0
[8]	1.50−2.75 / 60	38.5−41.5	8−11	71.4−84.0
[9]	1.40−2.60 / 60	39.0−40.0	10.2−12.2	60.0−70.0
[10]	0.60−1.00 / 50	45.2−46.9	10.7−12.4	66.0−87.8
This Work	1.30−2.70 / 70	39.8−42.0	9.8−12.0	55.8−69.7

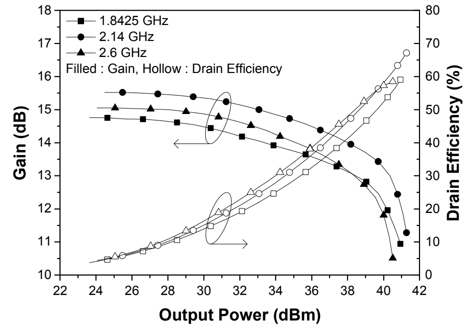

Fig. 7. Measured gain and efficiency performances at 1.8425, 2.14, and 2.6 GHz.

at 1.8425-GHz LTE (10-MHz BW 6.5-dB PAPR), 2.14-GHz WCDMA (5-MHz BW 7.0-dB PAPR), and 2.6-GHz m-WiMAX (10-MHz BW 8.5-dB PAPR) applications. For the signals with various BWs and PAPRs, HSA can efficiently operate by changing the reference value of the hysteresis comparator. The maximum output voltage of the HSA is 30 V. For the LTE, WCDMA, and m-WiMAX signals, the implemented HSA delivers the efficiencies of 67.9, 67.5, and 60% with the constant load impedance of 50 Ω, which is the average load impedance seen into the drain bias port of the implemented broadband saturated amplifier. The lower efficiency for the m-WiMAX signal is caused by the higher PAPR. The envelope signal applied to the amplifier is shaped to maximize PAE performance. Fig. 7 shows the measured efficiency and gain characteristics for a CW signal at the above three frequencies. the implemented amplifier provides the maximum efficiencies of 59.0, 67.1, and 58.5% for the frequencies at the saturated output power of 40.9, 41.3, and 40.5 dBm, respectively. Fig. 8 shows the measured output spectrums of the ET amplifiers before and after digital predistortion (DPD). The interlock experimental results are summarized in Table II. Since the ET amplifiers operate at the saturated region for all supply voltages, the gain performances are degraded. However, PAEs for LTE, WCDMA, and m-WiMAX applications are improved by 3.1, 4.2, and 1.7%, respectively, in comparison with the standalone PA. Moreover, by adopting the DPD technique, the linearity performances are meet to the system requirements.

IV. CONCLUSIONS

A multimode/multiband ET transmitter consisting of a HSA and a broadband saturated amplifier is presented. For the various wireless applications with different BW and PAPR, a highly efficient operation of HSA is accomplished by adapting the reference value of the hysteresis comparator. A saturated PA maintains high efficiency operation across the wide bandwidth without any special harmonic loads because the PA takes advantage of the nonlinear output capacitor to shape the voltage waveform. The fundamental load and source impedances are found from the load/source-pull methodology. Then, the broadband matching networks are synthesized by SRFT. For the bandwidth from 1.3 to 2.7 GHz, the measured

978-1-61284-757-3/11/$26.00 C2011 IEEE

TABLE II
ET PA MEASUREMENT SUMMARY

LTE Signal at 1.8425 GHz	Output Power (dBm)	Gain (dB)	DE (%)	PAE (%)	ACLR (7.50-MHz) (dBc)	ACLR (12.50-MHz) (dBc)
Standalone PA w/o DPD	34.99	13.29	30.48	29.05	–25.14	–32.24
ET PA w/o DPD	35.00	10.83	35.75	32.79	–26.93	–33.07
ET PA w/ DPD	34.72	10.62	35.21	32.16	–45.20	–46.00
WCDMA Signal at 2.14 GHz	Output Power (dBm)	Gain (dB)	DE (%)	PAE (%)	ACLR (2.50-MHz) (dBc)	ACLR (5.00-MHz) (dBc)
Standalone PA w/o DPD	35.00	14.18	34.34	33.02	–29.22	–38.00
ET PA w/o DPD	35.00	10.97	41.16	37.87	–28.74	–32.80
ET PA w/ DPD	34.73	10.60	40.79	37.24	–46.90	–47.50
m-WiMAX Signal at 2.6 GHz	Output Power (dBm)	Gain (dB)	DE (%)	PAE (%)	ACLR (5.32-MHz) (dBc)	ACLR (6.05-MHz) (dBc)
Standalone PA w/o DPD	33.00	13.88	28.18	27.03	–26.80	–29.20
ET PA w/o DPD	33.01	9.31	31.57	27.87	–21.45	–24.55
ET PA w/ DPD	32.89	8.93	32.97	28.75	–44.30	–45.40

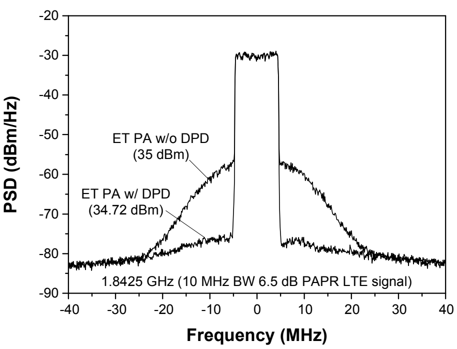

(a)

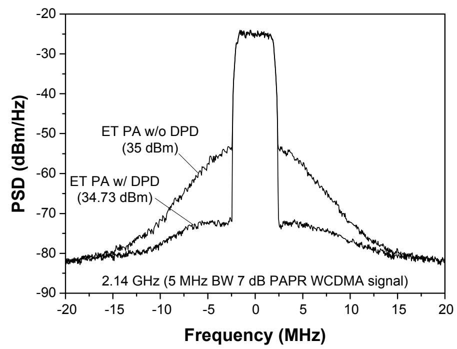

(b)

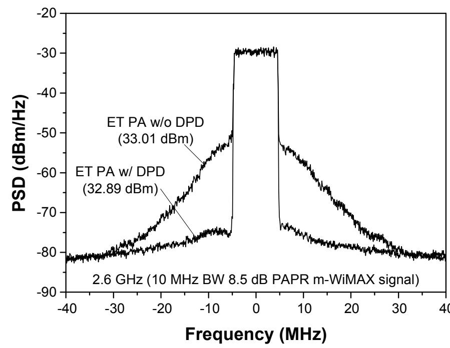

(c)

Fig. 8. Output spectrums of the ET amplifiers at (a) 1.8425, (b) 2.14, and (c) 2.6 GHz before and after DPD.

output power, DE, and PAE performances are between 39.8–42.0 dBm, 55.8–69.7%, and 51.2–65.3%, respectively. The ET transmitter is demonstrated at 1.8425-GHz LTE, 2.14-GHz WCDMA, and 2.6-GHz m-WiMAX applications. The transmitter delivers the PAE of 32.16, 37.24, and 28.75% for LTE, WCDMA, and m-WiMAX applications, respectively. By adopting the DPD technique, the linearity performances are within the system requirements.

ACKNOWLEDGEMENT

This work was supported by the MKE(The Ministry of Knowledge Economy), Korea, under the ITRC(Information Technology Research Center) support program supervised by the NIPA(National IT Industry Promotion Agency)(NIPA-2010-(C1090-1011-0011)) and WCU(World Class University) program through the Korea Science and Engineering Foundation funded by the Ministry of Education, Science and Technology(Project No. R31-2010-000-10100-0).

REFERENCES

[1] S.C. Cripps, *RF Power Amplifiers for Wireless Communications*. 2nd ed. Norwood, MA: Artech House, 2006.

[2] W. H. Doherty, "A new high efficiency power amplifier for modulated waves," *Proc. IRE*, vol. 24, no. 9, pp. 1163–1182, Sep. 1936.

[3] J. Choi, D. Kim, D. Kang, and B. Kim, "A polar transmitter with CMOS programmable hysteretic-controlled hybrid switching supply modulator for multi-standard applications," *IEEE Trans. Microw. Theory Tech.*, vol. 57, no. 7, pp. 1675–1686, Jul. 2009.

[4] D. F. Kimball, J. Jeong, C. Hsia, P. Draxler, S. Lanfranco, W. Nagy, K. Linthicum, L. E. Larson, and P. M. Asbeck, "High-efficiency envelope-tracking W-CDMA base-station amplifier using GaN HFETs," *IEEE Trans. Microw. Theory Tech.*, vol. 54, no. 11, pp. 3848–3856, Nov. 2006.

[5] J. Moon, J. Kim, and B. Kim, "Investigation of a class-J power amplifier with a nonlinear C_{out} for optimized operation," *IEEE Trans. Microw. Theory Tech.*, vol. 58, no. 11, pp. 2800–2811, Nov. 2010.

[6] D. Y.-T. Wu, F. Mkadem, and S. Boumaiza, "Design of a broadband and highly efficient 45W GaN power amplifier via simplified real frequency technique," in *IEEE MTT-S Int. Microw. Symp. Dig.*, Jun. 2010, pp. 1090–1093.

[7] P. Saad, C. Fager, H. Cao, H. Zirath, and K. Andersson, "Design of a highly efficient 2–4-GHz octave bandwidth GaN-HEMT power amplifier," *IEEE Trans. Microw. Theory Tech.*, vol. 58, no. 7, pp. 1677–1685, Jul. 2010.

[8] A. A. Tanany, D. Gruner, A. Sayed, and G. Boeck, "Highly efficient harmonically tuned broadband GaN power amplifier," in *Proc. 40th Eur. Microw. Conf.*, Sep. 2010, pp. 5–8.

[9] P. Wright, J. Lees, J. Benedikt, P. J. Tasker, and S. C. Cripps, "A methodology for realizing high efficiency Class-J in a linear and broadband PA," *IEEE Trans. Microw. Theory Tech.*, vol. 57, no. 12, pp. 3196–3204, Dec. 2009.

[10] A. A. Tanany, A. Sayed, and G. Boeck, "Broadband GaN switch model class E power amplifier for UHF applications," in *IEEE MTT-S Int. Microw. Symp. Dig.*, Jun. 2009, pp. 761–764.